



Three-Dimensional Nano-displacement Measurement by Four-Beam Laser Interferometry

Xu Zhang^{1,2,3} · Zi Wang^{1,2,3} · Mengnan Liu^{1,2,3} · Zhengxun Song^{1,2,3} · Zuobin Wang^{1,2,3,4} · Litong Dong^{1,2,3}

Received: 5 January 2024 / Revised: 27 March 2024 / Accepted: 29 March 2024
© The Author(s) 2024

Abstract

A 3D nano-displacement measurement method, where the difference in phase between the beams in a four-beam laser interference is changed, is proposed. Simulation results demonstrate that the variation of phase difference causes the deviation of the interference pattern in the laser interference system. Based on this theory, we design and build a four-beam laser interference system. The corner cube prism in the optical path is shifted, and the phase of the beam is changed by applying different voltages to a piezoelectric stage. The phase difference is obtained by analyzing the lattice pattern with subpixel precision, and then the displacement is determined by correlation operation. The experimental measurement results are consistent with the theoretical analysis, thereby verifying the feasibility of this measurement method.

Highlights

1. The four-beam laser interference lattice pattern can achieve higher precision displacement measurement.
2. The 3D displacement measurement system of the four-beam laser interference can realize single-dimensional or multi-dimensional displacement measurement. At the same time, it provides a basis for micro-displacement measurement in various applications.
3. The specific pixels of the interference pattern are accurately located using the correlation operation to achieve precise measurement results and minimize errors.

Keywords Four-beam laser interferometry · Phase difference · 3D displacement · Correlation operation

1 Introduction

As one of the most basic geometric parameters, the accurate measurement of displacement is greatly important for researchers in various fields, promoting scientific developments [1, 2]. In recent years, with the rapid development of precision manufacturing and processing, particularly microelectronics [3], semiconductors [4], and other industries, enhanced precision displacement measurement technology has been highly required [5, 6]. Among them, laser interferometry has become an important technology in the field of ultra-precision measurement, given its advantages of large range, high resolution, noncontact and traceability, and applicability [7–9].

At present, the precision displacement measurement methods are mainly divided into three types: electrical, mechanical, and optical methods. Among them, the electrical measurement method is the most sensitive. However,

✉ Zuobin Wang
1561788492@qq.com

✉ Litong Dong
donglt@cust.edu.cn

¹ International Research Centre for Nano Handling and Manufacturing of China, Changchun University of Science and Technology, Changchun 130022, China

² Centre for Opto/Bio-Nano Measurement and Manufacturing, Zhongshan Institute of Changchun University of Science and Technology, Zhongshan 528437, China

³ Ministry of Education Key Laboratory for Cross-Scale Micro and Nano Manufacturing, Changchun University of Science and Technology, Changchun 130022, China

⁴ JR3CN & IRAC, University of Bedfordshire, Luton LU1 3JU, UK

its insulation treatment is remarkably complex, and it is greatly disturbed by electromagnetic fields. The mechanical measurement method has strong anti-interference ability, with limited measurement dynamic range, frequency range, and linear and low measurement accuracy [10]. The optical measurement method has the advantages of low time consumption and high precision; it is also widely used in close-range engineering measurements [11–13]. Laser interference displacement measurement technology (DMLI) uses laser wavelengths as a benchmark to sense the displacement information through the frequency and phase changes of the interference spot [14, 15]. At present, DMLI is widely used in precision displacement measurements [16], but most of them are only suitable for 1D and 2D displacement measurements without changing the structure of the optical path configuration. However, the actual displacement measurement extends beyond 1D and 2D limitations. Research on 3D displacement measurement promotes the development of high-precision manufacturing [17, 18].

In the last decades, various 3D displacement measurement systems have been developed. Ri et al. [19] developed a precise 3D displacement measurement system using a single Charge Couple Device (CCD) attached to a precision three-axis mobile stage. Broetto et al. [20] developed a compact electronic speckle interference system for measuring 3D displacement. The system uses a laser diode as the light source and two orthogonally arranged diffraction gratings to enable the measurement area to obtain a uniform optical path length. Hsieh et al. [21] proposed a composite speckle interferometry interferometer that can achieve remote measurements of the smallest three dimensions. Shen et al. [22] proposed an inventive laser self-mixing interferometer, which has a reflective 2D grating for 3D dynamic displacement sensing. Lu et al. [23] proposed a 3D displacement measurement system using a single illumination detection path. The compact optical system generated three different sensitivity vectors used for the online measurement of 3D displacement. To achieve 3D or multi-degree-of-freedom measurements, a relatively simple optical path system is designed by changing the existing optical path configuration [24, 25], and a noncontact measurement laser interference system is developed to achieve 3D and even multi-degree-of-freedom displacement measurements.

In this study, we propose a laser interferometry system for measuring 3D displacement. The proposed scheme uses a four-beam laser interference system to design the specific optical path configuration for 3D displacement measurement. Only one laser is required to achieve 3D displacement measurement independently and simultaneously. The effectiveness of the system for measuring 3D displacement was tested using a piezoelectric stage. The experimental results confirm that the system has the advantages of high measurement resolution,

high precision, and multi-dimension. The system design can realize 3D displacement measurement. At the same time, the configuration is simple and can be assembled and adjusted intrinsically, exhibiting great practicability.

2 Theory

To compute the intensity distribution of a four-beam interference, the beam can be approximated as a plane wave with the same wavelength and intensity. The time factor is neglected in the experiment, i.e., without regard to the variation of the beam with time. The plane wave equation along the arbitrary direction in space can be expressed as follows:

$$\mathbf{E}_n = A_n \cdot \mathbf{e}_n \cdot \exp [i \cdot \mathbf{K}_n (\mathbf{r} + \varphi_n)] \quad (1)$$

where A_n is the amplitude, \mathbf{e}_n and \mathbf{K}_n are the Hongjie polarization vector and the wave vector, respectively, \mathbf{r} is the unit vector of the plane wave in the propagation direction in space, and φ_n is the initial phase.

In Eq. (1), \mathbf{K}_n , \mathbf{e}_n , and \mathbf{r} can be expressed as

$$\mathbf{K}_n = (k \cdot \sin \theta_n \cdot \cos \Phi_n, k \cdot \sin \theta_n \cdot \sin \Phi_n, -k \cdot \cos \theta_n) \quad (2)$$

$$\mathbf{e}_n = \begin{pmatrix} -\cos \theta_n \cdot \cos \Phi_n \cdot \cos \Psi_n + \sin \Phi_n \cdot \sin \Psi_n \\ -\cos \theta_n \cdot \sin \Phi_n \cdot \cos \Psi_n - \cos \Phi_n \cdot \sin \Psi_n \\ -\sin \theta_n \cdot \cos \Psi_n \end{pmatrix} \quad (3)$$

$$\mathbf{r} = (x, y, z) \quad (4)$$

where $k = 2\pi/\lambda$, λ is the laser wavelength, θ_n is the incident angle of the laser beam, Φ_n is the azimuth angle of the beam, and Ψ_n is the polarization angle of the beam.

The laser intensity distribution of multi-beam interference can be expressed as:

$$\begin{aligned} I(\mathbf{r}) &= \left| \sum_{j=1}^N E_j \right|^2 \\ &= \sum_{j=1}^N E_{0j}^2 + 2 \sum_{i<j} E_{0i} E_{0j} e_{ij} \cos [(\mathbf{K}_i - \mathbf{K}_j) \cdot \mathbf{r} + (\varphi_{0i} - \varphi_{0j})] \end{aligned} \quad (5)$$

where $e_{ij} = \mathbf{e}_i \cdot \mathbf{e}_j$.

Under the condition of interference, the difference of phase and optical distance difference of coherent beam satisfy the following relationship.

$$\Delta\varphi = \varphi_{0i} - \varphi_{0j} = \frac{2\pi}{\lambda} \cdot \delta = \frac{2\pi}{\lambda} \cdot n_0 \cdot (l_i - l_j) \quad (6)$$

where l_i and l_j are the optical path of the i th and j th beams, δ is the optical path difference between any two beams, and n_0 is the refractive index of light in air, $n_0 = 1.00029$.

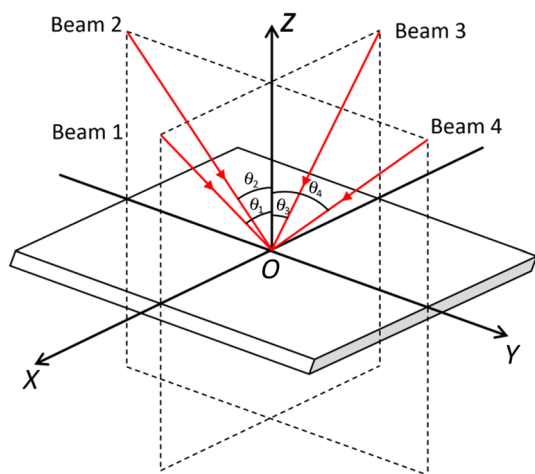


Fig. 1 Four-beam interference diagram

As shown in Fig. 1, the laser wavelength is 632.8 nm, and the intensity of the four beams is the same. The four beams of monochromatic coherent laser beams are incident from two orthogonal planes at $\theta_1, \theta_2, \theta_3,$ and θ_4 to form an interference. At the same time, it follows the spatial symmetrical configuration, and the azimuth angles are $\Phi_1=0^\circ, \Phi_2=90^\circ, \Phi_3=180^\circ,$ and $\Phi_4=270^\circ$. Equations (6) and (7) show that the initial phase difference $\Delta\varphi$ is the key factor in this experiment. The same polarization angles are selected to ensure that the amplitude of the interference field does not change with the difference in phase. Under this condition, the effect of the optical path on the four-beam interference pattern is observed by changing the phase difference between the beams.

According to these conditions, when $\theta_1=\theta_2=\theta_3=\theta_4=\theta,$ the four-beam interference in the x and y directions can be expressed as follows:

$$d_x = d_y = \frac{\lambda}{2 \sin \theta} \tag{7}$$

Figure 2 shows the simulation results. Beam 1 is considered the reference beam. The results shown in Fig. 2a–g illustrate that when the optical path of Beam 2 or Beam 4 changes, the variation of phase difference causes the vertical shift of the interference design. Figure 2a–e show that when the Beam 3 optical path changes, the change in the phase difference causes the interference pattern to shift horizontally.

Figure 2 shows the phase modulation lattice diagram and intensity curve. The figure indicates that the optical path changes in Beam 2 and Beam 4 affect the vertical shift of the interference pattern, and the optical path change in Beam 3 affects the horizontal shift of the interference pattern. The spatial symmetrical distribution of the four beams suggests that the two beams located in the same plane have the same moving direction of the pattern. Thus, the optical distance

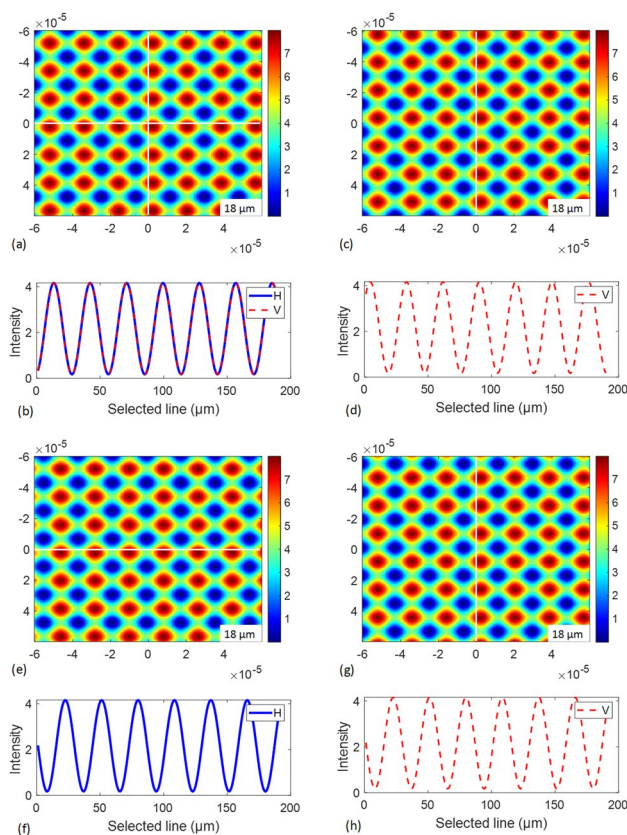


Fig. 2 Simulation of spatially symmetric four-beam interference ($\lambda = 632.8$ nm) on the $Z=0$ plane. The parameters of the four beams are $A_1:A_2:A_3:A_4=1 : 1 : 1 : 1, \theta=1^\circ,$ **a** shows the original four-beam interference pattern. **b** illustrates the intensity curve along the double arrow lines in **a**. H and V are the intensity curves in the horizontal and vertical directions, respectively. **c**, **e**, and **g** are the interferograms of Beam 2, Beam 3, and Beam 4, respectively, after the optical path is increased by 200 nm. **d**, **f**, and **h** represent the intensity curves along the double arrow lines in **c**, **e**, and **g**, respectively

difference of the two beams in the same plane cannot be obtained from a single lattice pattern. Consequently, the 3D phase information in the lattice pattern cannot be obtained. Figure 1 shows that beam 2 and beam 4 are in the yo z plane, and the optical path changes of these beams cannot be obtained from a lattice pattern. To solve this problem, two lattice patterns carrying 1D and 2D phase information can be selected for analysis. Therefore, the 2D phase information of the lattice pattern can be observed by changing the optical paths of Beam 2 and Beam 3 or Beam 3 and Beam 4 at the same time. Figure 3 shows the simulation results.

For the four-beam interference, the completely symmetrical interference results shown in Fig. 2a should be obtained. On this basis, a reference beam is established, and the interference results after shift are obtained by changing the optical path of the other beams. The amplitude and incident angle of the four beams in Figs. 2 and 3 are equal, and the

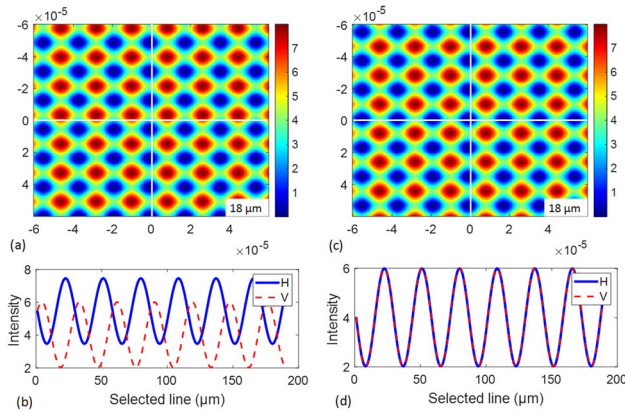


Fig. 3 Beam 2 and Beam 3 optical path increase of 200 nm interference pattern at the same time

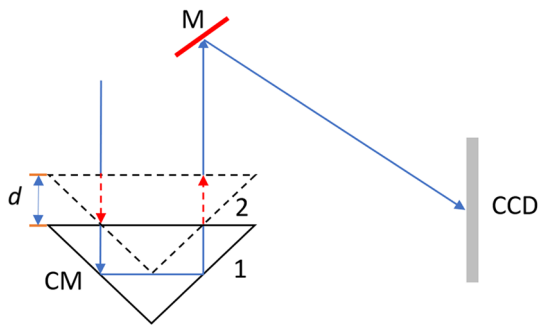


Fig. 4 Change in beam position caused by a piezoelectric stage, where *M* indicates mirror and *CM* is corner cube prism

azimuth angle follows the symmetrical configuration shown in Fig. 1. Here, their periods and intensity distributions are the same. The coherent beams interfere at the encounter point in a spatially symmetrical manner to avoid the modulation of the pattern, which is important for studying the change between the optical path of the beams and the shift of the interference pattern.

The relationship between the beam optical path and the interference pattern shift is verified in this four-beam interference system. The optical path of the coherent beam is changed using a piezoelectric ceramic actuator and a corner cube, as shown in Fig. 4.

In Fig. 4, the corner cube prism moves from position 1 to position 2 under the action of the piezoelectric ceramic actuator. Moreover, the moving distance is *d*, and then the optical path change under the corner cube prism is *2d*. When the beam is incident on the corner cube prism, the beam can return accurately at the same angle as the incident angle. The reflected light is always parallel to the incident light. When the light enters and leaves from the middle line of the corner cube prism, the optical path is

the largest at this time. Moving in the vertical direction of the light propagation, whether downward or upward, the optical path length of the light inside the corner cube prism decreases. It still causes the interference pattern to shift horizontally or vertically. According to Eq. (6), the relationship between the displacement and the phase difference ($\Delta\varphi$) can be obtained as follows:

$$\Delta\varphi = \frac{4\pi}{\lambda} \cdot n_0 \cdot d \tag{8}$$

In this system, the calculation of the phase difference directly affects the measurement accuracy. Correlation is a very important measurement method, and its research is constantly improved in scientific development. The correlation coefficient ρ_{xy} represents an important numerical characteristic of the similarity between two variables (*x*, *y*). The absolute value of ρ_{xy} represents the degree of correlation, and its sign indicates the direction of correlation; it is expressed as follows:

$$\rho_{xy} = \frac{\text{cov}(x,y)}{\sigma(x) \cdot \sigma(y)} \tag{9}$$

where $\text{cov}(x, y)$ is the covariance of variables *x* and *y*, $\sigma(x)$ and $\sigma(y)$ are the mean square deviations of variables *x* and *y*, respectively. When $\rho_{xy} = 0$, the two variables do not exhibit a linear relationship. When $|\rho_{xy}| = 1$, a linear relationship exists between the variables (*x*, *y*).

The correlation operation uses the correlation coefficient to determine the similarity of the two images; thus, the phase difference between the two images can be calculated by the correlation coefficient curves. The process of correlation operation is similar to that of convolution operation. It is equivalent to scanning another function *f* from the beginning to the end after translating one function *g* in the process. It reflects the similarity degree of function *g* and function *f* under different shifts. This similarity degree depends on their cross-correlation function values. The correlation operation reflects the degree of similarity between images and not the coordinates. Therefore, when the scan is completely coincident, the degree of similarity reaches the maximum, resulting in a correlation peak. In addition, the correlation operation presents a smoothing effect, which is equivalent to a low-pass filter and has good anti-noise performance. Generally, the fluctuation of the function itself will be smoothed after the correlation operation.

The phase difference between the lattice patterns of the 1D phase change can be calculated. Assuming that the reference image is $I_0(x, y)$ and the moving image is $I_k(x \pm t_0, y)$, then the correlation coefficient formula for solving autocorrelation and cross-correlation operations can be written as follows:

$$\rho_k(t_0) = \frac{\text{cov}[(I_0(x,y), I_k(x \pm t_0, y))]}{\sigma_{I_0} \cdot \sigma_{I_k}} \quad (10)$$

where I_0 and I_k represent the light intensity distribution of the two image modules, $\text{cov}[(I_0(x,y), I_k(x \pm t_0, y))]$ represents the covariance, and t_0 indicates the number of pixels that the image module moves. The symbol before t_0 depends on the directions of the moving image module, and σ_{I_0} and σ_{I_k} represent the standard variances.

Then, the 2D correlation coefficient equation of the lattice pattern can be written as follows:

$$\rho_k(t_1, t_2) = \frac{\text{cov}[(I_0(x,y), I_k(x \pm t_1, y \pm t_2))]}{\sigma_{I_0} \cdot \sigma_{I_k}} \quad (11)$$

where t_h and t_v represent the number of pixels, where the image module moves horizontally and vertically, respectively.

The correlation coefficient curve of phase change is drawn by Matlab, and the position where the correlation coefficient is zero is selected as the linear interpolation point. The difference Δx between the two curves at the zero-crossing point is the phase difference between the two dot matrix patterns calculated by interpolation operation. At this time, the phase difference is calculated in pixels. Equation (12) converts Δx into the phase difference in the unit of degree and then combines Eq. (6) to solve the optical path variation of the beam, that is, the displacement variation. The phase difference can be calculated by the following:

$$\Delta\varphi = \frac{\Delta x}{T} \cdot 2\pi \quad (12)$$

where T is the period of the correlation coefficient curve.

3 Experiment

The simulation results suggest that in the four-beam interference, as long as the azimuth angles are set to be $\Phi_1 = 0^\circ$, $\Phi_2 = 90^\circ$, $\Phi_3 = 180^\circ$, and $\Phi_4 = 270^\circ$, the phase change only exhibits the horizontal or vertical shift of the interference pattern and does not change the period and strength distribution of the interference field. As shown in Fig. 5, we build the 3D measurement system of a four-beam interference and observe the interference pattern changes to obtain the phase change information. The light source of the system is a linearly polarized He–Ne laser with a wavelength of 632.8 nm and a power of 1 mW. The beam is divided into four equal-intensity beams through a half-wave plate, a polarizer, and four-beam splitters. One beam is used as a reference beam, and the three other beams are reflected by an adjustable plane mirror to a 3D structure constructed with a corner cube prism. The last four beams are reflected to the CCD (SHL-500 W, resolution of 2048×1536 and effective pixel

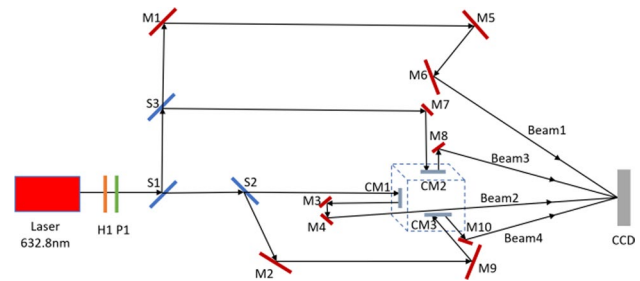


Fig. 5 Four-beam interferometry schematic, where H indicates the half-wave plate, P is polarizer, S is beam splitter, M is mirror, and CM is corner cube prism

size of $2.2 \mu\text{m}$) through a plane mirror to obtain an interference pattern. CCD can capture the changing interference lattice pattern for our application and restore the details and color of the laser light accurately. The design of the optical path determines the spatial angle and the incident angle of laser interference. This optical path can also be used to study the interference of two beams and three beams.

According to Fig. 5, the setting parameters required for the four-beam interference are selected. In the experiment, a 3D measurement system is constructed using three corner cube prisms of CM1, CM2, and CM3. The corner cube prism has a small displacement introduced with a piezoelectric stage. Using the characteristics of the reflected light from the corner cube prism parallel to the incident light, the beam is still collimated after entering and leaving the corner cube prism. By adjusting the plane mirror, the incident angles of the four beams are equal and set to 1° , and the azimuth space is symmetrical. Beam 1 and Beam 3 are in the vertical plane, Beam 2 and Beam 4 are in the horizontal plane, Beam 1 is used as the reference beam, and Beam 2, Beam 3, and Beam 4 constitute the 3D measurement beams. Finally, the four beams interfere on the CCD and are recorded.

Figure 6 shows the experimental results of the four-beam interference obtained by CCD in the experiment. Figure 6a illustrates the original interference result without any change in the optical path of the beam. The period in the horizontal direction is $d_x = 40 \mu\text{m}$, and that in the vertical direction is $d_y = 44 \mu\text{m}$. Figure 6b shows the experimental result after changing the optical path of Beam 2 in the x direction. Figure 6c illustrates the interference pattern after changing the optical paths of two beams in the y and z directions simultaneously. The comparison of the interference results in Fig. 6a, b indicate that after the optical path of Beam 4 increases, the interference pattern shifts upward in the vertical direction. The comparison between Fig. 6a, c shows that when the optical paths of Beam 4 and Beam 3 in the y and z directions increase, the interference pattern shifts downward in the vertical direction and then to the left in

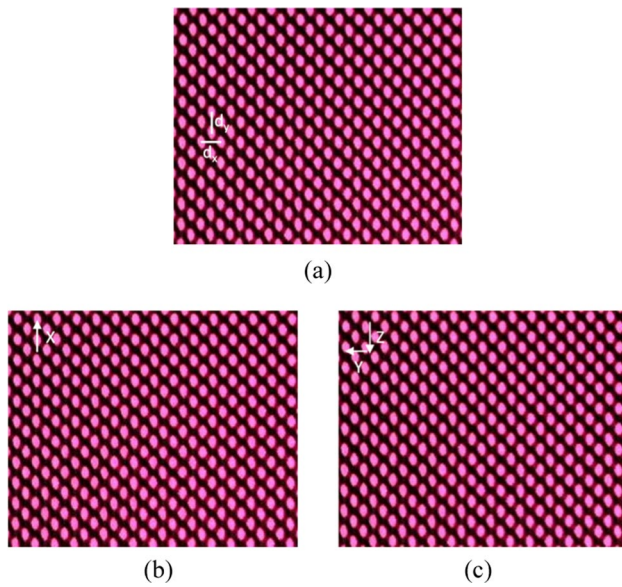


Fig. 6 **a** Experimental results of spatial symmetric four-beam interference. **b** Optical path of the beam in the x direction changes. **c** Optical path of the beam in the y and z directions changes simultaneously

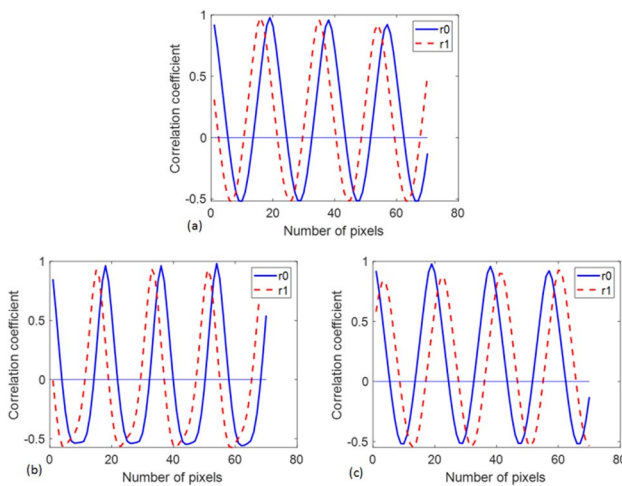


Fig. 7 Correlation coefficient curves of the interference patterns in Fig. 6: **a** x direction; **b** z direction; **c** y direction

the horizontal direction. The four-beam interference pattern obtained by the experiment is consistent with the theoretical simulation results. Although the light intensity is not uniform due to the influence of stray light, we found that the shift of the interference pattern induced by the optical path change of the beam is consistent with the theoretical simulation results, thereby confirming the feasibility of the experimental scheme.

Figure 7 shows the correlation coefficient curves before and after the change in the experimental pattern. Figure 7a illustrates the phase curve shift in the vertical direction of

Fig. 6b and 7b, c are the phase curve shifts in the horizontal and vertical directions of Fig. 6c, respectively. The phase difference between any two lattice patterns is obtained by linear interpolation using the zero-crossing point of the correlation coefficient curve. According to Eq. (7), the 3D displacement variation can be calculated. The displacements in the x , y , and z directions are measured at 99, 86, and 108 nm, respectively. It can realize a large range displacement measurement of 40–44 μm . A small deflection of the corner cube during the movement can induce a change in the incident angle and azimuth angle of the measured beam. After the change, the shape and period of the interference pattern will change, and the two lattice patterns with different shapes and periods cannot be processed by correlation operations.

4 Conclusion

The laser interference displacement measurement system has been developed to achieve 3D and high-precision measurements. Therefore, 3D nano-displacement measurements in the four-beam interference are studied. Through theoretical analysis, the phase change affects the shift of the interference pattern in the horizontal and vertical directions. According to this characteristic, the displacement measurement is introduced into the phase change to design a 3D displacement measurement system. Based on the principle of four-beam interference, the scheme is discussed from the theoretical and experimental aspects. To study the influence of phase change on the interference pattern, the displacement variation can be determined by the shift of the interference pattern. In summary, a 3D nano-displacement measurement system based on laser interference is proposed to realize 3D displacement measurements independently and simultaneously. The lattice pattern formed by this method can be offset from the horizontal and vertical directions, and multiple sets of displacement information can be obtained from a pair of lattice patterns to reduce the system error introduced in the acquisition process. The experimental results are consistent with the simulation results. The experimental results confirm the effectiveness of the method in measuring x -axis, y -axis, and z -axis displacements. The proposed method can be applied to high-precision 3D measurement systems in the fields of microelectronics and semiconductors.

Acknowledgements This work was supported by National Key R&D Program of China (No. 2023YFE0108900), Horizon Europe Program (L4DNANO No.101086227), Jilin Provincial Science and Technology Program (Nos. 20210101393JC, 20210101069JC, 20210101038JC, 2020C022-1, 20190201287JC and 20190702002GH), and “111” Project of China (No. D17017).

Author Contributions All authors read and approved the final manuscript.

Availability of Data and Materials The authors declare that all data supporting the findings of this study are available within the article.

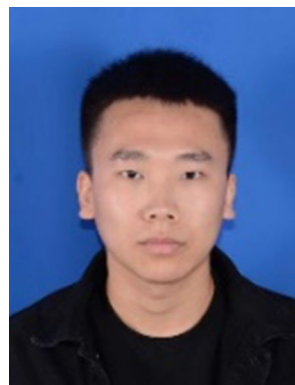
Declarations

Competing interests The authors declare that they have no conflicts of interest.

Open Access This article is licensed under a Creative Commons Attribution 4.0 International License, which permits use, sharing, adaptation, distribution and reproduction in any medium or format, as long as you give appropriate credit to the original author(s) and the source, provide a link to the Creative Commons licence, and indicate if changes were made. The images or other third party material in this article are included in the article's Creative Commons licence, unless indicated otherwise in a credit line to the material. If material is not included in the article's Creative Commons licence and your intended use is not permitted by statutory regulation or exceeds the permitted use, you will need to obtain permission directly from the copyright holder. To view a copy of this licence, visit <http://creativecommons.org/licenses/by/4.0/>.

References

- Sun B, Zheng G, Zhang X (2021) Application of contact laser interferometry in precise displacement measurement. *Measurement* 174:108959
- Li D, Li Q (2022) Quadrature phase detection based on a laser self-mixing interferometer with a wedge for displacement measurement. *Measurement* 202:111888
- Gao H, Yang D, Hu X (2023) High-precision micro-displacement measurement in a modified reversal shearing interferometer using vortex beams. *Opt Commun* 537:129454
- Cheng C, Xiao W, Ou Y (2023) Displacement measurement of sub-nanometer resolution using space-domain active fiber cavity ring-down technology. *Opt Laser Technol* 158:108815
- Hoang AT, Vu TT, Pham DQ (2023) High precision displacement measuring interferometer based on the active modulation index control method. *Measurement* 214:112819
- Kumar ASA, Anandan N, George B (2019) Improved capacitive sensor for combined angular and linear displacement sensing. *IEEE Sens J* 19(22):10253–10261
- Deng Z, Liu Z, Jia X (2019) Dynamic cascade-model-based frequency-scanning interferometry for real-time and rapid absolute optical ranging. *Opt Express* 27(15):21929–21945
- Chang D, Sun Y, Wang J (2023) Multiple-beam grating interferometry and its general Airy formulae. *Opt Lasers Eng* 164:107534
- Zhang S, Liu Q, Lou Y (2022) Simultaneous phase detection of multi-wavelength interferometry based on frequency division multiplexing. *J Lightwave Technol* 40(15):4990–4998
- Yang S, Zhang G (2018) A review of interferometry for geometric measurement. *Meas Sci Technol* 29(10):102001
- Zhang Z, Dong L, Ding Y (2017) Micro and nano dual-scale structures fabricated by amplitude modulation in multi-beam laser interference lithography. *Opt Express* 25(23):29135–29142
- Zhu J, Wang L, Wu J (2023) Achieving 1.2 fm/Hz^{1/2} displacement sensitivity with laser interferometry in two-dimensional nanomechanical resonators: pathways towards quantum-noise-limited measurement at room temperature. *Chin Phys Lett* 40(3):038102
- Hsieh HL, Kuo PC (2020) Heterodyne speckle interferometry for measurement of two-dimensional displacement. *Opt Express* 28(1):724–736
- Lu H, Hao Y, Guo C (2022) Nano-displacement measurement system using a modified orbital angular momentum interferometer. *IEEE J Quantum Electron* 58(2):1–5
- Serrano-Garcia DI, Toto-Arellano NI, Parra-Escamilla GA (2018) Multiwavelength wavefront detection based on a lateral shear interferometer and polarization phase-shifting techniques. *Appl Opt* 57(24):6860–6865
- Yan L, Chen B, Wang B (2017) A differential Michelson interferometer with orthogonal single frequency laser for nanometer displacement measurement. *Meas Sci Technol* 28(4):045001
- Yan H, Chen LY, Long J (2022) 3D shape and displacement measurement of diffuse objects by DIC-assisted digital holography. *Exp Mech* 62(7):1119–1134
- Xu Z, Wang Z, Chen L (2021) Two-dimensional displacement sensor based on a dual-cavity Fabry-Perot interferometer. *J Lightwave Technol* 40(4):1195–1201
- Ri S, Yoshida T, Tsuda H (2022) Optical three-dimensional displacement measurement based on moiré methodology and its application to space structures. *Opt Lasers Eng* 148:106752
- Broetto FZ, Schajer GS (2022) A compact ESPI system for measuring 3D displacements. *Exp Mech*: 1–12
- Hsieh HL, Sun BY (2021) Development of a compound speckle interferometer for precision three-degree-of-freedom displacement measurement. *Sensors* 21(5):1828
- Shen Z, Guo D, Zhao H (2021) Laser self-mixing interferometer for three-dimensional dynamic displacement sensing. *IEEE Photon Technol Lett* 33(7):331–334
- Lu M, Wang S, Bilgeri L (2018) Online 3D displacement measurement using speckle interferometer with a single illumination-detection path. *Sensors* 18(6):2018
- Wang X, Kondo M, Hanawa M (2023) Experimental demonstration of non-contact and quasi OPD-independent nanoscale-displacement measurement by phase-diversity optical digital coherent detection and comb filtering. *Opt Express* 31(2):2566–2583
- Hsieh HL, Pan SW (2015) Development of a grating-based interferometer for six-degree-of-freedom displacement and angle measurements. *Opt Express* 23(3):2451–2465



Xu Zhang is currently a master student in Changchun University of Science and Technology. His research interest is the 3D nano-displacement measurement technology.



Zi Wang is currently a master student in Changchun University of Science and Technology. Her research interest is the application of multi-beam interferometry in 3D profile measurement.



Zuobin Wang is a professor, and the director of international research centre for nano handling and manufacturing of China, in Changchun University of Science and Technology. His research is in the fields of laser nano-manufacturing, robot nano-manipulation and nano-measurement technology.



Mengnan Liu is currently a post-doctoral researcher in Changchun University of Science and Technology. Her research interest is the application of micro-nano lithography technology and microfluidic chips.



Litong Dong is a research assistant at Changchun University of Science and Technology. She mainly focuses on the laser interference lithography, micro-nano manufacturing, functional surface research and application.



Zhengxun Song is currently a professor at Changchun University of Science and Technology. His work focuses on nano-manipulation, nano-manufacturing and systems, and optical & wireless communications.